



Published in final edited form as:

Anesthesiology. 2018 October ; 129(4): 744–755. doi:10.1097/ALN.0000000000002368.

Anesthetics have different effects on the electrocorticographic spectra of wildtype and mitochondrial mutant mice

Charles William Carspecken, M.D.^{1,2,*}, Sirisak Chanprasert, M.D.^{1,3,*}, Franck Kalume, Ph.D.^{1,4,#}, Margaret M. Sedensky, M.D.^{1,2,#}, and Philip G. Morgan, M.D.^{1,2,#}

¹Center for Integrative Brain Research, Seattle Children's Research Institute, Seattle, WA 98195, USA

²Department of Anesthesiology and Pain Medicine, University of Washington, Seattle, WA 98195, USA

³Division of Medical Genetics, Department of Medicine, University of Washington, Seattle, WA 98195, USA

⁴Department of Neurological Surgery, University of Washington, Seattle, WA 98195, USA

Abstract

Background—Knockout of the mitochondrial protein *Ndufs4* (*Ndufs4(KO)*) in mice causes hypersensitivity to volatile anesthetics but resistance to ketamine. We hypothesized that electrocorticographic changes underlying the responses of *Ndufs4(KO)* to volatile anesthetics and to ketamine would be similar in mutant and control mice.

Methods—Electrocorticographic recordings at equipotent volatile anesthetic concentrations were compared between genotypes. In separate studies, control and cell type-specific *Ndufs4(KO)* mice were anesthetized with intraperitoneal ketamine to determine their ED50s.

Results—*Ndufs4(KO)* did not differ from controls in baseline electrocorticography (N=5). Compared to baseline, controls exposed to isoflurane (EC50) lost power (expressed as mean baseline($\mu V^2/Hz$); mean isoflurane ($\mu V^2/Hz$)) in delta (2.45; 0.50), theta (1.41; 0.16), alpha (0.23; 0.05), beta (0.066; 0.016), and gamma (0.020; 0.005) frequency bands (N=5). Compared to baseline, at their isoflurane EC50, *Ndufs4(KO)* maintained power in delta (1.08; 1.38), theta (0.36; 0.26), and alpha (0.09; 0.069) frequency bands but decreased in beta (0.041; 0.023) and gamma (0.020; 0.0068) frequency bands (N=5). Similar results were seen for both genotypes in halothane. VGLUT2-specific *Ndufs4(KO)* mice were markedly resistant to ketamine (ED50; 125 mg/kg) compared to control mice (ED50; 75mg/kg) (N=6). At their respective ED₉₅s for ketamine, mutant

Corresponding Author: Philip G. Morgan, M.D., Room 923, ¹Center for Integrative Brain Research, Seattle Children's Research Institute, 1900 9th Ave., Seattle, WA 98195, USA.

*these authors contributed equally to this work

#these authors contributed equally to this work

Clinical trial number and registry. Not applicable

Prior Presentations. This work will be presented in part at the 2017 meeting of the American Society of Anesthesiologists, Boston MA.

Conflicts of Interest. The authors declare no competing interests.

(N=5) electrocorticography spectra showed a decrease in power in the beta (0.040; 0.020) and gamma (0.035; 0.015) frequency bands not seen in controls (N=7).

Conclusions—Significant differences exist between the electrocorticographies of mutant and control mice at equipotent doses for volatile anesthetics and ketamine. The energetic state specifically of excitatory neurons determines the behavioral response to ketamine.

Keywords

Ndufs4, mitochondria; volatile anesthetics; ketamine; electroencephalography; spectral analysis

Introduction

The molecular mechanisms of action of volatile anesthetics (VAs) are not fully elucidated^{1–3}. Ketamine, like the VAs, is a complete general anesthetic. Ketamine is an NMDA receptor (NMDAR) antagonist^{4,5}, but also affects other ion channels^{6,7}. Moreover, competitive inhibitors with greater affinity for the NMDAR than ketamine do not cause the anesthetized state⁸. Thus, like the VAs, the mechanism of action for ketamine is not understood.

Disruption of a specific step of mitochondrial electron transfer, complex I, causes hypersensitivity to VAs in humans, nematodes, and mice^{9–11} suggesting an evolutionarily conserved connection between neuronal metabolism and sensitivity to VAs. However, the mechanisms linking mitochondrial function to anesthetic sensitivity are unclear. Mice carrying the knockout (KO) of the nuclear gene *Ndufs4*, which encodes an 18kDa protein of complex I of the mitochondrial electron transport chain, have a striking 3-fold increase in sensitivity to VAs. This is the largest change in VA anesthetic sensitivity measured in a mammal¹¹. Surprisingly, *Ndufs4* homozygous knock out (KO) mice are also resistant to ketamine requiring ~50% higher doses to achieve loss of the righting reflex (LORR)¹¹.

Electroencephalography monitors electrical activity within the brain as oscillations that reflect voltage changes from currents and local field potentials generated by neurons¹². There is a growing body of evidence to suggest that different anesthetic agents alter or disrupt the oscillations produced by the brain, and unique patterns of the electrocorticogram (ECoG) can be associated with the anesthetized state caused by specific anesthetics^{13–15}. An ECoG power spectrum depicts the power distributions of individual frequency components. Similar analyses of EEG spectra have yielded systems level insights into the phenomenon of general anesthesia^{16,17}. Characteristic spectral patterns have been associated both with different planes of anesthesia as well as different types of anesthetic agents^{13,14}. While the spectral changes under various anesthetics have been explored, it is unclear how disruption of neuronal aerobic metabolism affects field oscillatory behavior detected with the ECoG. Given that VAs directly inhibit complex I^{18–20} and that the *Ndufs4(KO)* decreases complex I activity in neurons by ~50%¹², we hypothesized that the VAs would induce similar changes in the ECoG spectra in control and KO animals at equipotent concentrations. We studied the ECoG patterns of KO and control mice exposed to halothane and isoflurane.

Restricting the *Ndufs4* mutation to glutamatergic neurons gives the full increase in sensitivity to VAs^{11,21}. Here we determined whether the resistance of *Ndufs4(KO)* to ketamine was also dependent on glutamatergic-specific KO of the gene. Finally, we determined whether the ECoG patterns in KO and control mice were similar when anesthetized by ketamine. We hypothesized that ketamine would induce similar changes in the ECoG spectra in control and KO animals at equipotent doses.

The goal of these studies were to establish if the anesthetized state in the *Ndufs4(KO)* is similar to that of control mice. If differences exist between the two genotypes, they may help determine which aspects of the ECoG spectra are important for anesthesia.

Material and Methods

Ethics Statement

The study was carried out in strict accordance with the recommendations in the Guide of the Care and Use of Laboratory Animals of the National Institute of Health. All animal experiments were performed with the approval of the Animal Care and Use Committee of the Seattle Children's Research Institute (IACUC protocol). All surgeries were performed humanely with all efforts to minimize pain and suffering.

Generation and Maintenance of Mouse Lines

Mice were maintained on a standard rodent diet with 12 hours dark-light cycle at 22°C. Water and food were available *ad libitum*. Both male and female mice were used for all experiments. Mice heterozygous for *Ndufs4* null allele (*Ndufs4^{-/+}*) in a C57BL/6 genetic background were crossed to produce wild-type (*Ndufs4^{+/+}*), heterozygous (*Ndufs4^{-/+}*) and knock-out [*Ndufs4^{-/-}*, *KO* or *Ndufs4(KO)*] animals. The offspring genotype was determined by polymerase chain reaction. Only heterozygous (*Ndufs4^{-/+}*) mice were used for the control group.

Cell Specific *Ndufs4(KO)* Ketamine Exposure

Cell specific lines were generated and genotyped as previously described^{11,21,22} and were compared to their siblings heterozygous for *Ndufs4^{lox}* and for the *Cre* driver. No animals were excluded from analysis. The numbers of animals scored for each anesthetic and genotype are given in the legends to figure 5. The offspring genotype was determined by polymerase chain reaction. Cre expression was localized to CNS cell types as previously described²³. Animals were genotyped using tail DNA and tested for absence of ectopic recombination at the end of the experiment using CNS DNA. Loss of righting reflex was determined as previously described.¹¹

Surgery

Mice underwent survival surgery at ages P28–32 to implant ECoG and EMG electrodes under isoflurane anesthesia with additional subcutaneous bupivacaine for analgesia as described previously²⁴. Using aseptic technique, a midline incision was made anterior to posterior to expose the cranium. Fine (diameter: 0.127mm bare; 0.178 mm coated) silver wires were placed through cranial holes created with a fine cutting needle and fixed in place

with cyano-acrylate adhesive. ECoG electrodes were placed at visually identified locations – left and right frontal cortices, approximately 1 mm anterior to the bregma and 3mm lateral to the sagittal suture. EMG electrodes were placed in back muscles. A reference electrode was placed at the midline cerebellum and a ground electrode was placed subcutaneously over the back and the skin was closed with sutures. Electrode impedances were typically < 10 kΩ. 1 mg/kg of 0.25% bupivacaine in sterile saline was injected subcutaneously immediately after surgery. The mice were recovered for 1 hour and then transferred to their cages. Carprofen MediGel was put in the animal cages for 48 hours.

ECoG recording

Twenty-four to 48 hours after ECoG electrodes placement, the mice were exposed to anesthetic while the ECoG was monitored as previously described^{24,25}. Briefly, all biopotential signals were acquired at 1-KHz sampling rate and 100X Gain. ECoG signals were processed offline with a 1–70 Hz bandpass filter and a 60 Hz trap filter to reduce line noise if necessary. The EMG signals were processed offline with a 3 Hz high-pass filter. ECoG patterns were evaluated prior to recording to ensure complete recovery from anesthesia. A digital Video/ECoG/EMG recording system (LabChart, ADInstruments, Australia) was used to record EMG/ECoGs from freely-behaving awake or anesthetized mice. All bioelectrical signals were acquired at 1-KHz sampling rate and 100X Gain. ECoG signals were processed offline with a 1–70 Hz bandpass filter and a 60 Hz trap filter to reduce line noise if necessary. Mice were exposed to stepwise increases in VA concentration (8–10 minutes in 0.2%–0.3% increments) to reach their EC₅₀ for loss of response to tail clamp (0.4% for KO and 1.2% for controls) as well as ~1.5% X EC₅₀ (0.6% for KOs and 2% for controls). Sensitivity to the second VA was assessed 24 hours later in an identical manner. Isoflurane and halothane were done in alternate order in sequential mice. For all anesthetic ECoGs (VA and ketamine) the baseline ECoG for each anesthetic was determined by an unexposed ECoG done immediately prior to the anesthetic exposure. Blinding of the observer to mouse genotype was not possible as the mutant and control mice are visibly distinct. Since ECoG data was obtained independently of genotype, blinding was not necessary. Based on previous experience with the complete KO, an N=5 was felt to be sufficient to obtain significance for biologically relevant changes.

For ketamine studies, age-matched wild type and *Ndufs4(KO)* mice underwent ECoG implantation as per the VAs. Twenty-four to 48 hours after ECoG electrodes placement, the mice were injected with intraperitoneal racemic ketamine (Ketaved, Vedco, MO) at their ED₉₅s (determined previously as 100mg/kg for wild type, and 150mg/kg for KO¹¹). Animals underwent surgery at P28–30 and had ECoG recorded in awake and ketamine anesthetized states at their respective ED₉₅ dose. Both controls and KOs were sacrificed after experiment completion of ketamine or VA experiments. As for volatile anesthetics, based on previous experience with the complete KO, an N=5 was felt to be sufficient to obtain significance.

Statistics

After steady state exposure to equipotent doses of anesthetics, average power spectral analyses were performed by Fast Fourier Transform and results were compared between

anesthetic and awake states. Each ECoG tracing was inspected for signal quality and noise contamination in IGOR Pro 6 (Wavemetrics Lake Oswego, OR). The ratio of averaged power spectral density in the anesthetized and awake animal were calculated for each animal at the appropriate anesthetic concentration then pooled for analysis. For the graphs of power vs Hz, values were pooled in 1Hz bins, 0.1–1Hz represented at 1Hz, 1–2Hz at 2Hz and continuing in that pattern until 58–59Hz represented at 59Hz. 60Hz values were omitted due to high background signal.

Data are reported as mean \pm standard deviation (SD). Comparisons of spectral ratio data across five ECoG frequency ranges (delta 1–4Hz, theta 4–8Hz, alpha 8–13Hz, beta 13–30Hz, and gamma 31–59Hz) were made after each group was tested with a two-way Analysis of Variance (ANOVA). Since there were 5 groups to be tested with ANOVA (the five different frequency ranges, delta, theta, alpha, beta and gamma), we applied a Bonferroni correction to a p value threshold for ANOVA statistical significance of 0.01, changing the threshold for an acceptable ANOVA significance to $0.01/4=0.0025$. If the ANOVA significance reached that value, we tested the individual treatment groups in pairs comparing the anesthetic treated groups to the untreated group of the same genotype. Comparisons of power in each frequency between the paired groups were done using paired two-sided Student's t-test assuming unequal variance. Since, in volatile anesthetic experiments, there were four concentration groups for the controls and three for the KOs, we again used a Bonferroni correction to our basic limit of $p=0.01$. The correction was $0.01/3$ (0.003) for the controls and $0.01/2$ (0.005) for the KOs. For the ketamine studies, there were only a treated and untreated group at each frequency range. We therefore used a Bonferroni correction for the number of frequency ranges to use a $p<0.01/4=0.0025$ as a cutoff for significance for a two-way ANOVA. The only comparisons made for all tests, other than the baseline comparisons (Figure 2), were within a single genotype but at different anesthetic concentrations. While, in all studies, we did not compare power densities between different genotypes, such a comparison was done at baseline to establish the similarities of the two genotypes to each other. Since that led to an implied comparison between the genotypes in all further studies, the use of a two-way ANOVA is the most conservative approach to determine significance within groups. For all experiments, $n=5$ mice except the ketamine control, $n=7$. Results of all ANOVA tests and t-tests when indicated are shown in Table S1; p values are first number, ANOVA tests in parentheses.

Dose response curves for ketamine were constructed as follows using matched controls for each cell-specific *Ndufs4(KO)* line. For each curve shown in Figure 5, blue squares and blue solid lines reflect data points for the respective cell-specific *Ndufs4(KO)* strains. Similarly, red squares and red solid line reflect the data points for control mice used for those specific experiments. Green and magenta smoothed lines are the best fit lines fit to the data points. The curve fits for the loss of righting reflex (LORR) dose response curves were constructed as an interpolation of a standard sigmoidal curve using a four parameter logistic equation of the form $Y=Bottom + (Top-Bottom)/(1+10^{((LogEC50-X)*HillSlope)})$. Magenta and green dotted lines reflect the 95% confidence intervals for the interpolated fits.

During peer review, at the reviewer's request, sample sizes were increased from $n=4$ to $n=5$ for the isoflurane and halothane exposure groups. However, no further adjustments were

made for the repeated analysis of the enhanced sample sizes other than an altered Bonferroni correction due to the larger sample sizes.

Results

Baseline ECoG

There were no statistically significant differences in average power densities of individual frequency ranges or 5 frequency bands between the two genotypes at baseline (Figures 1, 2). In the control mice (N=5), the average power densities were: 2.04 $\mu\text{V}^2/\text{Hz}$ in the delta frequency band; 1.17 $\mu\text{V}^2/\text{Hz}$ in the theta frequency band; 0.26 $\mu\text{V}^2/\text{Hz}$ the alpha frequency band; 0.68 $\mu\text{V}^2/\text{Hz}$ in the beta frequency band; and 0.020 $\mu\text{V}^2/\text{Hz}$ in the gamma frequency band. In *Ndufs4(KO)* mice (N=5), the average power densities were: 1.37 $\mu\text{V}^2/\text{Hz}$ (p=0.08 compared with the control value) in the delta frequency band; 0.54 $\mu\text{V}^2/\text{Hz}$ (p=0.11) in theta frequency band; 0.16 $\mu\text{V}^2/\text{Hz}$ (p=0.06) in the alpha frequency band; 0.054 $\mu\text{V}^2/\text{Hz}$ (p=0.14) in the beta frequency band; and 0.021 $\mu\text{V}^2/\text{Hz}$ (p=0.73) in the gamma frequency band (Figure 2C). None of the differences between KO and control reached the Bonferroni corrected p-value limit of 0.0025. (Table S1)

Isoflurane

Since the *Ndufs4(KO)* mice are anesthetized at 0.6% isoflurane and 0.6% halothane while controls are not, we first characterized the differences in their respective ECoGs at those concentrations of anesthetic. We then compared the ECoGs in the two genotypes at anesthetic concentrations normalized to their EC₅₀s or 1.5XEC₅₀s. To make the comparisons between genotypes, for the KO we used the EC₅₀ as 0.4% (both isoflurane and halothane) and 1.5XEC₅₀ as 0.6% (for both VAs). For the control we used the EC₅₀ as 1.2% (both VAs) and 1.5XEC₅₀ as 1.8% (for both VAs).

Controls—In the control mice, the average power densities in all frequency bands at 0.6% isoflurane were not statistically significant from those of the unexposed animals (Figure 3A,B; blue, black curves, Table S1). The average power densities decreased significantly at the EC₅₀ for isoflurane (Figure 3A,B; blue, gray curves, 1.2% isoflurane) when compared to baseline in delta (2.45 $\mu\text{V}^2/\text{Hz}$ and 0.50 $\mu\text{V}^2/\text{Hz}$; p<0.0001), theta (1.41 $\mu\text{V}^2/\text{Hz}$ and 0.16 $\mu\text{V}^2/\text{Hz}$; p<0.0001), alpha (0.23 $\mu\text{V}^2/\text{Hz}$ and 0.05 $\mu\text{V}^2/\text{Hz}$; p<0.0001), beta (0.066 $\mu\text{V}^2/\text{Hz}$ and 0.016 $\mu\text{V}^2/\text{Hz}$; p<0.0001), and gamma (0.020 $\mu\text{V}^2/\text{Hz}$ and 0.005 $\mu\text{V}^2/\text{Hz}$; p<0.0001) frequency bands (Figure 3E,F; blue, green bars). At 1.5XEC₅₀ (Figure 3A,B; blue, green curves; 1.8% isoflurane), the average power densities decreased further across all frequency bands when compared to baseline; delta (0.13 $\mu\text{V}^2/\text{Hz}$; p<0.0001), theta (0.073; p<0.0001), alpha (0.021 $\mu\text{V}^2/\text{Hz}$; p<0.0001), beta (0.007 $\mu\text{V}^2/\text{Hz}$; p<0.0001), and gamma (0.004 $\mu\text{V}^2/\text{Hz}$; p<0.0001) (Figure 3G,H; blue, green bars).

Ndufs4(KO)—At the EC₅₀ for *Ndufs4(KO)* in isoflurane (Figure 3C,D; red, grey curves; 0.4% isoflurane), the average power densities were unchanged in the delta (1.08 $\mu\text{V}^2/\text{Hz}$ and 1.38 $\mu\text{V}^2/\text{Hz}$; p=0.64), theta (0.36 $\mu\text{V}^2/\text{Hz}$ and 0.26 $\mu\text{V}^2/\text{Hz}$; p=0.48), and alpha (0.09 $\mu\text{V}^2/\text{Hz}$ and 0.069 $\mu\text{V}^2/\text{Hz}$; p=0.14) frequency bands but decreased in the beta (0.041 $\mu\text{V}^2/\text{Hz}$ and 0.023 $\mu\text{V}^2/\text{Hz}$; p<0.0001) and gamma (0.020 $\mu\text{V}^2/\text{Hz}$ and 0.0068 $\mu\text{V}^2/\text{Hz}$;

$p < 0.0001$) frequency bands (Figure 3E,F; red, purple bars). At 1.5XEC₅₀ (Figure 3C,D; red, green curves; 0.6% isoflurane), the mutant had significant changes only in the beta ($0.016 \mu\text{V}^2/\text{Hz}$; $p < 0.0001$) and gamma ($0.0054 \mu\text{V}^2/\text{Hz}$; $p < 0.0001$) frequency bands compared to baseline (Figure 3G,H; red, purple bars). Power in the delta, theta, and alpha ranges were not changed from baseline at either concentration of isoflurane.

Genotype comparisons—In summary, comparing the *patterns* of changes in Figure S2, at their respective EC₅₀s and 1.5XEC₅₀s for isoflurane, the decrease in total power across all frequencies was greater in the control than in the mutant. The differences between genotypes were noted especially in the lower frequencies.

Halothane

Controls—In the control mice, the average power densities in all frequency bands at 0.6% halothane were not statistically significant from those of the unexposed animals (Figure 4A,B; blue, black curves, Table S1). At the EC₅₀ for halothane (Figure 4A,B; blue, gray curves, 1.2% halothane) the average power densities decreased significantly in all frequency bands: delta ($1.62 \mu\text{V}^2/\text{Hz}$ and $0.74 \mu\text{V}^2/\text{Hz}$; $p = 0.0008$), theta ($0.93 \mu\text{V}^2/\text{Hz}$ and $0.29 \mu\text{V}^2/\text{Hz}$; $p < 0.0001$), alpha ($0.28 \mu\text{V}^2/\text{Hz}$ and $0.075 \mu\text{V}^2/\text{Hz}$; $p < 0.0001$), beta ($0.087 \mu\text{V}^2/\text{Hz}$ and $0.027 \mu\text{V}^2/\text{Hz}$; $p < 0.0001$), and gamma ($0.020 \mu\text{V}^2/\text{Hz}$ and $0.009 \mu\text{V}^2/\text{Hz}$; $p < 0.0001$) frequency bands (Figure 4E,F; blue, green bars). At 1.5XEC₅₀ (Figure 4A,B; blue, green curves; 1.8% halothane), when compared to baseline, the average power densities decreased further across all frequency bands; delta ($0.23 \mu\text{V}^2/\text{Hz}$, $p < 0.0001$), theta ($0.066 \mu\text{V}^2/\text{Hz}$, $p < 0.0001$) alpha ($0.020 \mu\text{V}^2/\text{Hz}$; $p < 0.0001$) beta ($0.009 \mu\text{V}^2/\text{Hz}$, $p < 0.0001$), and gamma ($0.0043 \mu\text{V}^2/\text{Hz}$; $p < 0.0001$) frequency bands (Figure 4G,H; blue, green bars).

Ndufs4(KO)—In *Ndufs4(KO)*, at the EC₅₀ for halothane (Figure 4C,D; red, grey curves; 0.4% halothane), the average power densities were decreased significantly only in the alpha ($0.18 \mu\text{V}^2/\text{Hz}$ and $0.08 \mu\text{V}^2/\text{Hz}$; $p = 0.002$), beta ($0.06 \mu\text{V}^2/\text{Hz}$ and $0.03 \mu\text{V}^2/\text{Hz}$; $p < 0.0001$) and gamma ($0.022 \mu\text{V}^2/\text{Hz}$ and $0.014 \mu\text{V}^2/\text{Hz}$; $p < 0.0001$) frequency bands (Figure 4E,F; red, purple bars). At 1.5XEC₅₀ (Figure 4C,D; red, green curves; 0.6% halothane), when compared to baseline, there was a significant change in the alpha ($0.062 \mu\text{V}^2/\text{Hz}$; $p = 0.002$), beta ($0.024 \mu\text{V}^2/\text{Hz}$; $p < 0.0001$) and gamma ($0.006 \mu\text{V}^2/\text{Hz}$; $p < 0.0001$) frequency bands (Figure 4G,H; red, purple bars).

Genotype comparisons—In summary, at their respective EC₅₀s for halothane, both control and KO had similar decreases in power across the higher frequency bands. At their respective 1.5XEC₅₀s for halothane, the decrease in total power across all frequencies was greater in the control than in the mutant. As with isoflurane, the differences between genotypes were noted especially in the lower frequencies.

Ketamine

Cell-specific *Ndufs4(KO)* Ketamine Sensitivity—Earlier studies showed that the VA hypersensitivity of *Ndufs4(KO)* was dependent on cell specific loss of the gene in glutamatergic neurons.²¹ We first determined if ketamine sensitivity also was dependent on cell-specific *Ndufs4(KO)*. Using loss of righting reflex (LORR) as the endpoint, we

compared the sensitivity to ketamine of control mice with that of mice with *Ndufs4* knocked out selectively in GABAergic neurons (*GABA-(KO)*), VGLUT2-positive glutamatergic neurons (*VGLUT2-(KO)*) or cholinergic neurons (*CHAT-(KO)*). VGLUT2-(KO) mice (ED₅₀ 125 ± 2 mg/kg) were markedly resistant to ketamine compared to control mice (ED₅₀ 75 ± 1.5 mg/kg; p<0.001), similar to the total KO mice (ED₅₀ 100 ± 2 mg/kg). GABAergic-specific *Ndufs4(KO)* (ED₅₀ 70 ± 5 mg/kg; p=0.86) and cholinergic-specific *Ndufs4(KO)* mice (ED₅₀ 90 ± 4 mg/kg; p=0.76) were not resistant to ketamine compared to the control mice (Figure 5). All mice appeared behaviorally normal until approaching the doses needed for LORR

Genotype specific changes in ECoG patterns during ketamine exposure—

Similar to our reasoning for the volatile anesthetics, we then compared the ECoGs for wild type and global KO mice at their respective ED₉₅s for ketamine.

Controls—In the control mice, the average power densities at the ketamine ED₉₅ (100mg/kg) (Figure 6A,B; blue, red curves) were not statistically significant from those of the unexposed animals in the delta (2.40 μV²/Hz and 2.56 μV²/Hz; p=0.89), theta (0.47μV²/Hz and 0.44 μV²/Hz; p=0.91), alpha (0.11μV²/Hz and 0.07 μV²/Hz; p=0.05), beta (0.031 μV²/Hz and 0.016μV²/Hz; p=0.06) and gamma (0.023 μV²/Hz and 0.013μV²/Hz; p=0.075) frequency bands (Figure 6E,F; blue, green bars).

Ndufs4(KO)—In *Ndufs4(KO)*, the average power densities at the ketamine ED₉₅ (150mg/kg) (Figure 6C,D; blue, black curves) were not statistically significant from those of the unexposed animals in the delta (1.25 μV²/Hz and 1.78 μV²/Hz; p=0.19), theta (0.39 μV²/Hz and 0.36 μV²/Hz; p=0.89) and alpha ranges (0.12 μV²/Hz and 0.12; p=0.092; p=0.37) (Figure 6E,F; red, purple bars). The average power densities were decreased significantly from baseline only in the beta (0.040 μV²/Hz and 0.020 μV²/Hz; p<0.0001) and gamma (0.035 μV²/Hz and 0.015 μV²/Hz; p<0.0001) frequency bands (Figure 6E,F; red, purple bars).

Genotype comparisons—In summary, at their respective EC₉₅s, control and KO had similar responses in the delta, theta, and alpha frequency ranges but differed in the upper frequencies (beta and gamma ranges) in that the control did not change while the KO decreased in power in those frequencies while the controls did not. Ketamine resistance tracks with loss of NDUFS4 in glutamatergic neurons.

Discussion

These data demonstrate significantly different neurophysiologic signatures equipotent doses of VAs between wild type and *Ndufs4(KO)* mice, an animal with known mitochondrial dysfunction. The differences are discussed below for each type of anesthetic.

Volatile Anesthetics

We hypothesized that when the concentrations of VAs reach their respective EC₅₀s, both mutant and control ECoGs would be similarly affected in frequency ranges necessary for maintenance of consciousness. At their EC₅₀s for each VA, control animals had significantly

lower power densities across all frequency bands than they did at baseline. These broad decreases were more pronounced at 1.5XEC50 for each VA. In contrast, the mutant animals maintained their power densities close to baseline values in the low power frequency range (delta, theta) in isoflurane at both the EC₅₀ and 1.5XEC50. In halothane, the control again had broad decreases in power in all frequency ranges at the EC₅₀. In the KO the decreases only reached significance in the alpha, beta and gamma frequency ranges. In addition, only the control mice had further decreases as the concentrations were raised to 1.5XEC50. Therefore, there are fundamental differences in the response of the two genotypes to concentrations of anesthetic at doses matched for potency.

Since mutant mice have very low EC₅₀s for both VAs¹¹, we hypothesized that we would see changes in the ECoGs of mutant mice at lower concentrations of VAs than in control mice. These changes would be interpreted as the marker of the anesthetized state in the mutant but not the control. At 0.6% isoflurane or halothane concentrations, no significant differences were noted in any frequency ranges in the ECoGs from control mice. In the mutant, power in alpha, beta and gamma frequency ranges were decreased at both 0.6% isoflurane and halothane. However, power in delta and theta ranges were maintained in both anesthetics despite animals being anesthetized. In humans, others have noted that, especially in anterior regions of the brain, power in the delta frequencies is maintained or even increased, during onset of volatile anesthetic action^{26–28}. While we did not do an exhaustive characterization of the sensitivity of the lower frequencies to anesthetic concentrations and we only placed single leads bilaterally, our results are in general agreement with those earlier studies. In fact, the KO maintained power in the lower frequencies even at anesthetizing concentrations. Losses of power in the lower frequencies are not necessary for the anesthetized state. These results are in agreement with earlier studies that arousal has been correlated with increased power in higher frequency ranges^{29–31}.

Previous studies in humans have shown that in volatile anesthetics at or near EC₅₀s, power is shifted from the higher frequencies (beta and gamma), to the lower ranges (delta, theta and alpha)^{14,32}. We did not see such a shift; rather we saw a broad decrease in power at all frequencies. However, the loss was more significant in the upper ranges such that a spectral presentation may have shown increased *relative* power in the theta or alpha ranges. It has also been noted that as consciousness is lost, there is a loss of functional connectivity between different regions of the brain (reviewed in³³). With our experimental setup, we were unable to determine whether such connectivity was affected.

The pattern of changes seen with volatile anesthetics in humans is similar to that of propofol and has been interpreted to indicate that the predominate effect of volatile agents is at the GABA receptor. We would caution that these similarities may indicate that similar neuronal networks are affected but not that identical or even similar molecular targets are involved. Our results are consistent with the possibility of a primary mitochondrial target for volatile anesthetics since both mutant and control lose power in the upper ranges despite being anesthetized at widely disparate concentrations; however, these results do not rule out other potential molecular targets for volatile agents.

Ketamine

Similar to earlier responses with volatile anesthetics, loss of *Ndufs4* in glutamatergic neurons is sufficient to cause resistance to ketamine. During sedation with ketamine, increases in gamma and beta frequency power spectra have been identified previously and thought to be due to anti-NMDA mediated disinhibition of pyramidal neurons^{15,34} as well as blocking fast-spiking cortical interneurons³⁵. In this manner, the reported EEG patterns following low dose ketamine are distinct from those seen with anesthetizing doses of volatile anesthetics and GABA_A-receptor agonists. ECoG or EEG patterns during higher dosing with ketamine causing the anesthetized state have not been well described. We measured no significant changes in the ECoGs of control mice when comparing baseline to anesthetizing doses of ketamine. However, the mutant ECoG decreased in power in the beta and gamma frequency ranges. Therefore, maintenance of power in the upper frequencies may not be necessary for the anesthetized state since the mutant is anesthetized in spite of a decrease in beta and gamma frequency oscillatory behavior.

Ketamine is associated with increased cerebral glucose utilization at subanesthetic doses³⁶ and a decrease in inhibitory tone with decreased GABA release³⁷. The relative resistance of the mutant to ketamine may result from the decrease in power in the higher frequencies resulting from circuit disruptions in cortical and subcortical sites³⁸. Although untested in this study, is it possible that the intercortical connectivity that produces ketamine anesthesia is not possible when pyramidal neurons in the mitochondrial mice are unable to mount a sufficiently excitatory response. However, it is important to note that there is no evidence that ketamine is an effective inhibitor of mitochondrial function. Therefore, the effect of *Ndufs4(KO)* may be an indirect one on an energetic state necessary for ketamine induced sedation rather than on a ketamine target such as the NMDA receptor or HCN1 channels.

Conclusion

In this study, we identified the characteristic changes in ECoG patterns induced by two VAs (isoflurane and halothane) as well as ketamine. Depression of ECoG power is relatively spared in the lower frequencies for the mutant compared to the control at equipotent concentrations of VAs. The decreases in power in the higher frequencies in the mutant at low concentrations of VAs indicates that these changes may be sufficient to cause the anesthetized state. In contrast, when exposed to equipotent doses of ketamine, ECoG power in the higher frequencies is maintained in controls but decreases in the mutant. These data suggest that increased power in the higher frequencies is not necessary for the anesthetizing effects of ketamine.

Supplementary Material

Refer to Web version on PubMed Central for supplementary material.

Acknowledgments

The authors thank Beatrice Predoi M.D., Center for Integrative Brain Research, Seattle Children's Research Institute, for assistance with mouse care and genotyping.

Funding. CWC was supported by the Department of Anesthesiology and Pain Medicine Bonica Scholar Program. SC was supported by the NW Mitochondrial Research Guild. MMS and PGM were supported by NIH grant R01GM105696 and by the NW Mitochondrial Research Guild. FK was supported by NIH/NINDS Grant R01NS102796, by the CURE Epilepsy Research Grant, and by Ellenbogen Chair UW Neurosurgery Research Funds.

References

1. Humphrey JA, Sedensky MM, Morgan PG. Understanding anesthesia: making genetic sense of the absence of senses. *Hum Mol Genet.* 2002; 11:1241–9. [PubMed: 12015284]
2. Campagna JA, Miller KW, Forman SA. Mechanisms of actions of inhaled anesthetics. *N Engl J Med.* 2003; 348:2110–24. [PubMed: 12761368]
3. Franks NP. General anaesthesia: from molecular targets to neuronal pathways of sleep and arousal. *Nat Rev Neurosci.* 2008; 9:370–86. [PubMed: 18425091]
4. Anis NA, Berry SC, Burton NR, Lodge D. The dissociative anaesthetics, ketamine and phencyclidine, selectively reduce excitation of central mammalian neurones by N-methyl-aspartate. *Br J Pharmacol.* 1983; 79:565–75. [PubMed: 6317114]
5. Orser BA, Pennefather PS, MacDonald JF. Multiple mechanisms of ketamine blockade of N-methyl-D-aspartate receptors. *Anesthesiology.* 1997; 86:903–17. [PubMed: 9105235]
6. Zhou C, Douglas JE, Kumar NN, Shu S, Bayliss DA, Chen X. Forebrain HCN1 channels contribute to hypnotic actions of ketamine. *Anesthesiology.* 2013; 118:785–95. [PubMed: 23377220]
7. Petrenko AB, Yamakura T, Sakimura K, Baba H. Defining the role of NMDA receptors in anesthesia: are we there yet? *Eur J Pharmacol.* 2014; 723:29–37. [PubMed: 24333550]
8. Daniell LC. The noncompetitive N-methyl-D-aspartate antagonists, MK-801, phencyclidine and ketamine, increase the potency of general anesthetics. *Pharmacol Biochem Behav.* 1990; 36:111–5. [PubMed: 2190239]
9. Kayser EB, Morgan PG, Sedensky MM. GAS-1: a mitochondrial protein controls sensitivity to volatile anesthetics in the nematode *Caenorhabditis elegans*. *Anesthesiology.* 1999; 90:545–54. [PubMed: 9952163]
10. Morgan PG, Hoppel CL, Sedensky MM. Mitochondrial defects and anesthetic sensitivity. *Anesthesiology.* 2002; 96:1268–70. [PubMed: 11981173]
11. Quintana A, Morgan PG, Kruse SE, Palmiter RD, Sedensky MM. Altered anesthetic sensitivity of mice lacking *Ndufs4*, a subunit of mitochondrial complex I. *PLoS One.* 2012; 7:e42904. [PubMed: 22912761]
12. Buzsaki G, Anastassiou CA, Koch C. The origin of extracellular fields and currents--EEG, ECoG, LFP and spikes. *Nat Rev Neurosci.* 2012; 13:407–20. [PubMed: 22595786]
13. Purdon PL, Pierce ET, Mukamel EA, Prerau MJ, Walsh JL, Wong KF, Salazar-Gomez AF, Harrell PG, Sampson AL, Cimenser A, Ching S, Kopell NJ, Tavares-Stoeckel C, Habeeb K, Merhar R, Brown EN. Electroencephalogram signatures of loss and recovery of consciousness from propofol. *Proc Natl Acad Sci U S A.* 2013; 110:E1142–51. [PubMed: 23487781]
14. Purdon PL, Sampson A, Pavone KJ, Brown EN. Clinical Electroencephalography for Anesthesiologists: Part I: Background and Basic Signatures. *Anesthesiology.* 2015; 123:937–60. [PubMed: 26275092]
15. Vlisides PE, Bel-Bahar T, Lee U, Li D, Kim H, Janke E, Tarnal V, Pichurko AB, McKinney AM, Kunkler BS, Picton P, Mashour GA. Neurophysiologic Correlates of Ketamine Sedation and Anesthesia: A High-density Electroencephalography Study in Healthy Volunteers. *Anesthesiology.* 2017; 127:58–69. [PubMed: 28486269]
16. Pavone KJ, Su L, Gao L, Eromo E, Vazquez R, Rhee J, Hobbs LE, Ibala R, Demircioglu G, Purdon PL, Brown EN, Akeju O. Lack of Responsiveness during the Onset and Offset of Sevoflurane Anesthesia Is Associated with Decreased Awake-Alpha Oscillation Power. *Front Syst Neurosci.* 2017; 11:38. [PubMed: 28611601]
17. Li D, Hambrecht-Wiedbusch VS, Mashour GA. Accelerated Recovery of Consciousness after General Anesthesia Is Associated with Increased Functional Brain Connectivity in the High-Gamma Bandwidth. *Front Syst Neurosci.* 2017; 11:16. [PubMed: 28392760]

18. Cohen PJ. Effect of anesthetics on mitochondrial function. *Anesthesiology*. 1973; 39:153–64. [PubMed: 4146381]
19. Harris RA, Munroe J, Farmer B, Kim KC, Jenkins P. Action of halothane upon mitochondrial respiration. *Arch Biochem Biophys*. 1971; 142:435–44. [PubMed: 4396285]
20. Kayser EB, Suthammarak W, Morgan PG, Sedensky MM. Isoflurane selectively inhibits distal mitochondrial complex I in *Caenorhabditis elegans*. *Anesth Analg*. 2011; 112:1321–9. [PubMed: 21467554]
21. Zimin PI, Woods CB, Quintana A, Ramirez JM, Morgan PG, Sedensky MM. Glutamatergic Neurotransmission Links Sensitivity to Volatile Anesthetics with Mitochondrial Function. *Curr Biol*. 2016; 26:2194–201. [PubMed: 27498564]
22. Kruse SE, Watt WC, Marcinek DJ, Kapur RP, Schenkman KA, Palmiter RD. Mice with mitochondrial complex I deficiency develop a fatal encephalomyopathy. *Cell Metab*. 2008; 7:312–20. [PubMed: 18396137]
23. Rossi J, Balthasar N, Olson D, Scott M, Berglund E, Lee CE, Choi MJ, Lauzon D, Lowell BB, Elmquist JK. Melanocortin-4 receptors expressed by cholinergic neurons regulate energy balance and glucose homeostasis. *Cell Metab*. 2011; 13:195–204. [PubMed: 21284986]
24. Kalume F, Westenbroek RE, Cheah CS, Yu FH, Oakley JC, Scheuer T, Catterall WA. Sudden unexpected death in a mouse model of Dravet syndrome. *J Clin Invest*. 2013; 123:1798–808. [PubMed: 23524966]
25. Kalume F, Oakley JC, Westenbroek RE, Gile J, de la Iglesia HO, Scheuer T, Catterall WA. Sleep impairment and reduced interneuron excitability in a mouse model of Dravet Syndrome. *Neurobiol Dis*. 2015; 77:141–54. [PubMed: 25766678]
26. MacIver MB, Bland BH. Chaos analysis of EEG during isoflurane-induced loss of righting in rats. *Front Syst Neurosci*. 2014; 8:203. [PubMed: 25360091]
27. Pilge S, Jordan D, Kreuzer M, Kochs EF, Schneider G. Burst suppression-MAC and burst suppression-CP(5)(0) as measures of cerebral effects of anaesthetics. *Br J Anaesth*. 2014; 112:1067–74. [PubMed: 24658022]
28. Gugino LD, Chabot RJ, Prichep LS, John ER, Formanek V, Aglio LS. Quantitative EEG changes associated with loss and return of consciousness in healthy adult volunteers anaesthetized with propofol or sevoflurane. *Br J Anaesth*. 2001; 87:421–8. [PubMed: 11517126]
29. Ma J, Leung LS. Limbic system participates in mediating the effects of general anesthetics. *Neuropsychopharmacology*. 2006; 31:1177–92. [PubMed: 16205783]
30. Leung LS, Petropoulos S, Shen B, Luo T, Herrick I, Rajakumar N, Ma J. Lesion of cholinergic neurons in nucleus basalis enhances response to general anesthetics. *Exp Neurol*. 2011; 228:259–69. [PubMed: 21295026]
31. Solt K, Cotten JF, Cimenser A, Wong KF, Chemali JJ, Brown EN. Methylphenidate actively induces emergence from general anesthesia. *Anesthesiology*. 2011; 115:791–803. [PubMed: 21934407]
32. Palanca BJA, Avidan MS, Mashour GA. Human neural correlates of sevoflurane-induced unconsciousness. *Br J Anaesth*. 2017; 119:573–582. [PubMed: 29121298]
33. Hudetz AG, Mashour GA. Disconnecting Consciousness: Is There a Common Anesthetic End Point? *Anesth Analg*. 2016; 123:1228–1240. [PubMed: 27331780]
34. Shaw AD, Saxena N, LEJ, Hall JE, Singh KD, Muthukumaraswamy SD. Ketamine amplifies induced gamma frequency oscillations in the human cerebral cortex. *Eur Neuropsychopharmacol*. 2015; 25:1136–46. [PubMed: 26123243]
35. Seamans J. Losing inhibition with ketamine. *Nat Chem Biol*. 2008; 4:91–3. [PubMed: 18202677]
36. Langsjö JW, Salmi E, Kaisti KK, Aalto S, Hinkka S, Aantaa R, Oikonen V, Viljanen T, Kurki T, Silvanto M, Scheinin H. Effects of subanesthetic ketamine on regional cerebral glucose metabolism in humans. *Anesthesiology*. 2004; 100:1065–71. [PubMed: 15114201]
37. Homayoun H, Moghaddam B. NMDA receptor hypofunction produces opposite effects on prefrontal cortex interneurons and pyramidal neurons. *J Neurosci*. 2007; 27:11496–500. [PubMed: 17959792]

38. Akeju O, Song AH, Hamilos AE, Pavone KJ, Flores FJ, Brown EN, Purdon PL. Electroencephalogram signatures of ketamine anesthesia-induced unconsciousness. *Clin Neurophysiol.* 2016; 127:2414–22. [PubMed: 27178861]

Author Manuscript

Author Manuscript

Author Manuscript

Author Manuscript

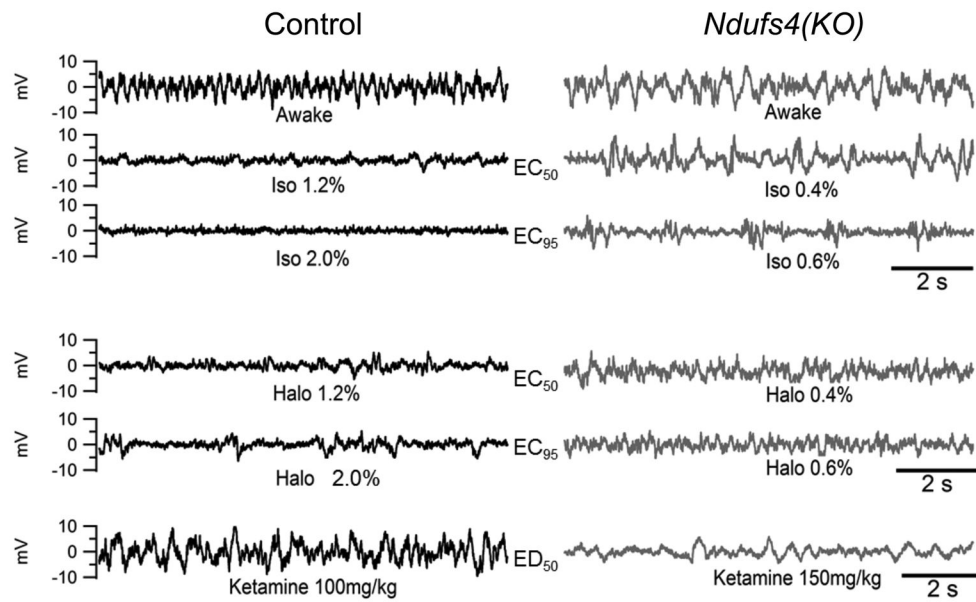


Figure 1. Representative 10 second EEG Tracings of KO and Control Mice in Awake and Anesthetized States

Halothane, Isoflurane and intraperitoneal racemic ketamine anesthetic EEG tracings are shown and paired at equipotent anesthetic concentrations. For each volatile anesthetic, tracings at concentrations corresponding to the EC_{50} and $1.5 \times EC_{50}$ are shown. For ketamine, tracings at doses corresponding to an ED_{95} are shown. Awake tracing is a representative tracing from a non-exposed EEG. EEGs are representative tracings for each concentration or dose.

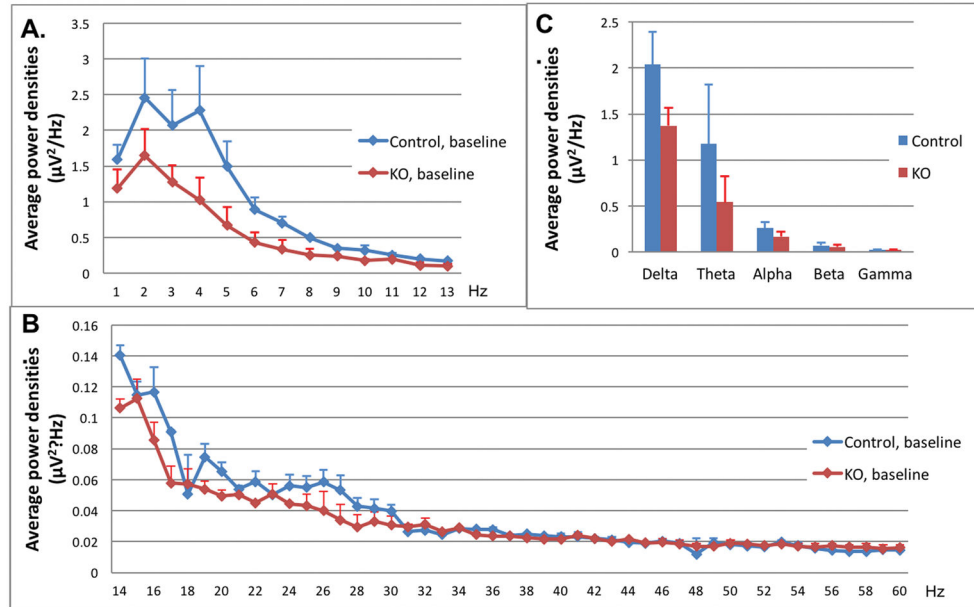


Figure 2. Power densities at baseline in control (blue line) and *Ndufs4*(KO) (red line) mice at baseline, in absence of anesthetic
A. Power densities for EEG activity in 1 Hz to 13 Hz band. **B.** Power densities from 13 Hz to 60 Hz. There were no significant differences between control and KO at any frequency. In A and B, each point is the mean of individual experiments. N=5 for both genotypes. Error bars are standard deviations. **C.** In each frequency band (delta, theta, alpha, beta, gamma), the average power densities are shown in control (blue bars) and *Ndufs4*(KO) (red bars). Bar values are the mean power in each of the respective labeled regions in panels A and B. Error bars represent standard deviations. As with values for individual frequencies there were no significant differences in the frequency ranges.

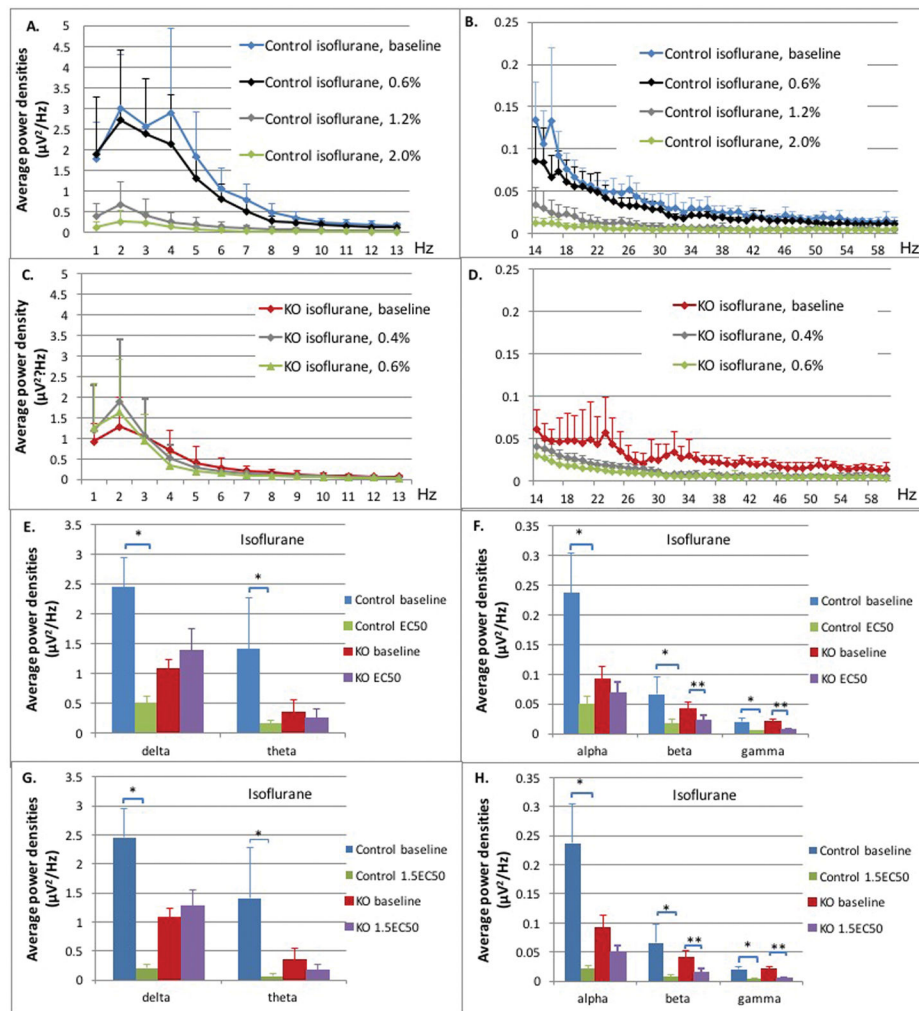


Figure 3. Control and *Ndufs4(KO)* mice in isoflurane

A–D: Average power densities plotted against frequency bands at different isoflurane concentrations. All points in curves in A–D represent an average of the bin including one Hz plotted at the upper value of that range. The value at 1Hz represents the bin from 0–1Hz, the 2Hz value represents the bin from 1–2Hz, for example. Data points represent the mean of all exposures ($n=5$ both genotypes). Error bars represent standard deviations. **(A)** Delta, theta and alpha frequency ranges from 1 Hz – 13 Hz, control mice. **(B)** Beta and gamma ranges from 14 Hz – 60 Hz, control mice. **(C)** Delta, theta and alpha frequency ranges from 1 Hz – 13 Hz, *Ndufs4(KO)*. **(D)** Beta and gamma ranges from 14 Hz – 60 Hz, *Ndufs4(KO)*. **E–F: Comparison for control and KO between baseline and isoflurane at EC₅₀s.** Average power densities in each frequency band at baseline and EC₅₀ isoflurane concentrations in control and KO groups: **(E)** delta and theta frequency bands; **(F)** alpha, beta and gamma frequency bands. Error bars are standard deviations. $N=5$ in all cases. Single and double stars for significance comparisons are only to indicate control and KO genotypes, respectively. **G–H: Comparison for control and KO between baseline and isoflurane at 1.5XEC₅₀s.** Average power densities in each frequency band at baseline and 1.5XEC₅₀ isoflurane concentrations in control and KO groups: **(G)** delta and theta frequency bands **(H)**

alpha, beta and gamma frequency bands. Error bars are deviations. N=5 in all cases. Single and double stars for significance comparisons are only to indicate control and KO genotypes, respectively.

Author Manuscript

Author Manuscript

Author Manuscript

Author Manuscript

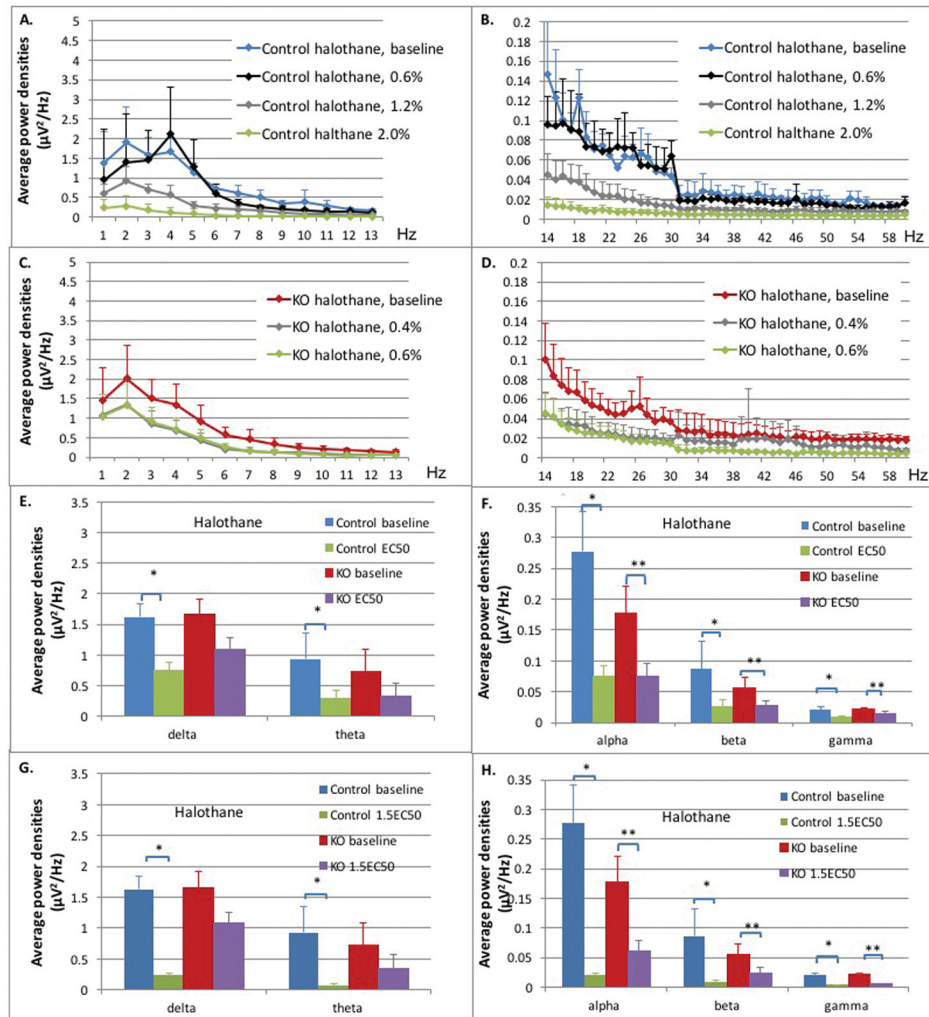


Figure 4. Control and *Ndufs4*(KO) mice in halothane

A–D: Average power densities plotted against frequency bands at different halothane concentrations. All points in curves in A–D represent an average of the bin including one Hz plotted at the upper value of that range. The value at 1Hz represents the bin from 0–1Hz, the 2Hz value represents the bin from 1–2Hz, for example. Data points represent the mean of all exposures ($n=5$ both genotypes). Error bars represent standard deviations. **(A)** Delta, theta and alpha frequency ranges from 1 Hz – 13 HZ, control mice. **(B)** Beta and gamma ranges from 14 Hz – 60 HZ, control mice. **(C)** Delta, theta and alpha frequency ranges from 1 Hz – 13 HZ, *Ndufs4*(KO). **(D)** Beta and gamma ranges from 14 Hz – 60 HZ, *Ndufs4*(KO). **E–F: Comparison for control and KO between baseline and halothane at EC₅₀s.** Average power densities in each frequency band at baseline and EC₅₀ halothane concentrations in control and KO groups: **(E)** delta and theta frequency bands; **(F)** alpha, beta and gamma frequency bands. Error bars are standard deviations. $N=5$ in all cases. Single and double stars for significance comparisons are only to indicate control and KO genotypes, respectively. **G–H: Comparison for control and KO between baseline and halothane at 1.5XEC₅₀s.** Average power densities in each frequency band at baseline and 1.5XEC₅₀ halothane concentrations in control and KO groups: **(G)** delta and theta frequency bands **(H)**

alpha, beta and gamma frequency bands. Error bars are deviations. N=5 in all cases. Single and double stars for significance comparisons are only to indicate control and KO genotypes, respectively.

Author Manuscript

Author Manuscript

Author Manuscript

Author Manuscript

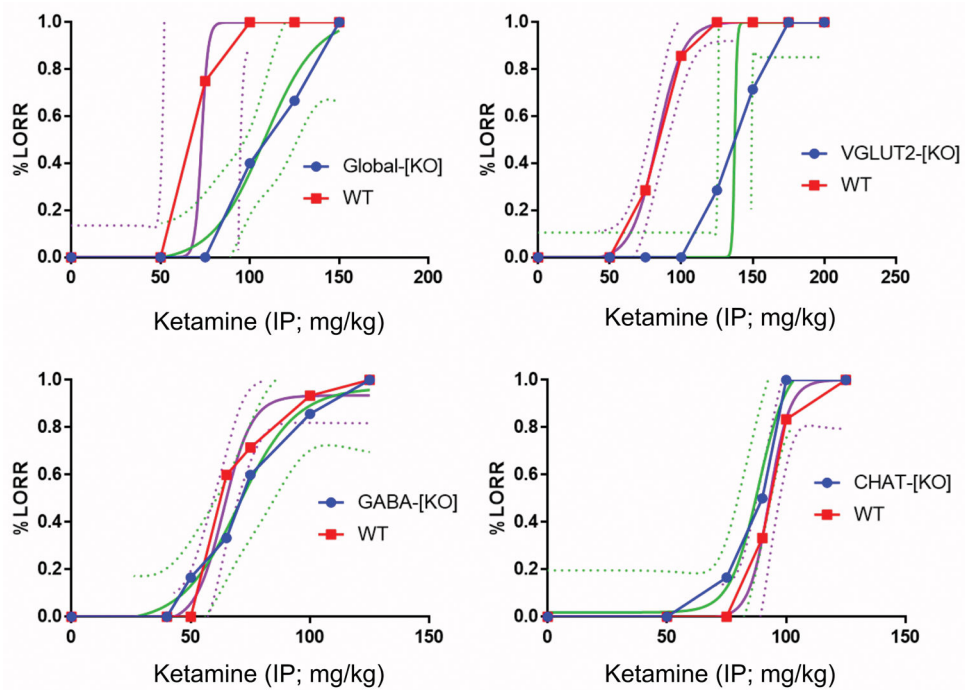


Figure 5. A–D. Dose response for ketamine using Loss of Righting Reflex (LORR) in global and cell-specific *Ndufs4(KO)* mice (A–D) compared to control mice
 Each graph shows the dose response curves to intraperitoneal ketamine for control (red) and KO (blue) mice as well as the related with variable slope and the interpolated curve fits (magenta, green solid lines) with the 95% confidence intervals (magenta, green dotted lines). **A.** Global *Ndufs4(KO)* mice compared to control mice. N=12 for the KO and 11 for controls. **B.** *Ndufs4(KO)* restricted to VGLUT2-positive glutamatergic neurons (*VGLUT2-(KO)*) compared to control. N=7 for each genotype. **C.** *Ndufs4(KO)* restricted to GABAergic neurons (*GABA-(KO)*) compared to control. N=7 for GABAergic KO, 15 for controls. **D.** *Ndufs4(KO)* restricted to cholinergic neurons (*CHAT-(KO)*) compared to control. N=6 for each genotype.

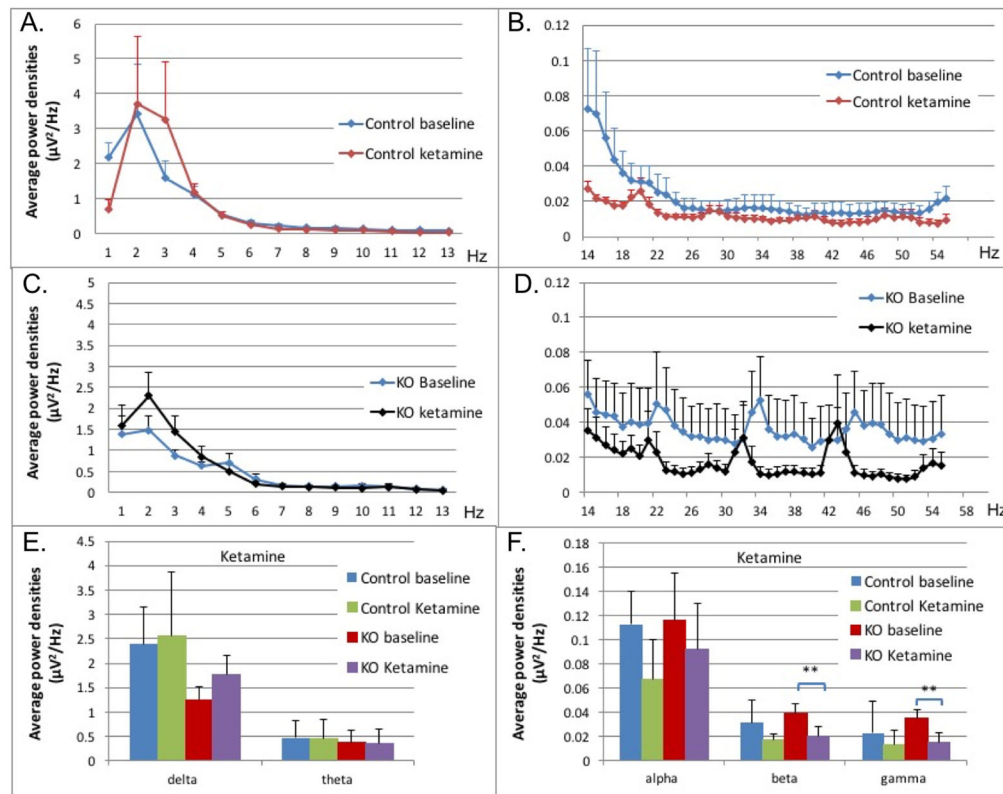


Figure 6. Control and *Ndufs4(KO)* mice and ketamine

A–D: Average power densities plotted against frequency bands at baseline and ED95 ketamine dose. All points in curves in A–D represent an average of the bin including one Hz plotted at the upper value of that range. The value at 1Hz represents the bin from 0–1Hz, the 2Hz value represents the bin from 1–2Hz, for example. Data points represent the mean of all exposures ($n=5$ for KO, $n=7$ for control). Error bars represent standard deviations. **(A)** Delta, theta and alpha frequency ranges from 1 Hz – 13 HZ, control mice. **(B)** The beta and gamma ranges from 14 Hz – 57 HZ, control mice (58–60 Hz was removed due to background interference). **(C)** Delta, theta and alpha frequency ranges from 1 Hz – 13 HZ, *Ndufs4(KO)*. **(D)** The beta and gamma ranges from 14 Hz – 57 HZ, *Ndufs4(KO)* (58–60 Hz was removed due to background interference). **E–F: Comparison for control and KO between baseline and ketamine at ED95s.** Average power densities in each frequency band in relation to ketamine at concentration at ED95 in control and KO groups: **(E)** delta and theta frequency bands **(F)**; alpha, beta, and gamma frequency bands. Error bars are standard errors of the mean. $N=5$ for mutant animals, $N=7$ for control animals. Brackets with stars indicate significance as described in Methods.